International Journal of Advance Research in Science and Engineering
Vol. No.4, Special Issue (01), September 2015
www.ijarse.com
IJARSE
ISSN 2319 - 8354

THERMOLUMINESCENCE STUDIES OF UV-IRRADIATED Y_20_3: DY^{+3}DOPED PHOSPHOR

Tarkeshwari Verma[1], Sadhana Agrawal[2]

[1,2]National Institute of Technology, Raipur C.G.(India)

ABSTRACT

The present paper reports thermo luminescence (TL) glow curves of Dy^{+3}-doped Y_20_3 phosphor with different ultraviolet (UV) exposure times and heating rates. The glow peak shows second-order kinetics of Dy^{+3}doped Y_20_3 and corresponding kinetic parameters, activation energy were evaluated using the peak-shape method. Calculations of trap depth were also carried out using peak shape method. The recorded glow curve shifts towards higher intensity with longer UV exposure time. Particle size and structure were verified by X-ray diffraction (XRD) pattern and morphology by scanning electron microscopy (SEM), Fourier transform infrared (FTIR) also use for characterization.

Keywords: Thermo luminescence (TL), Kinetic parameter ,Rare-earth-doped phosphor.

I. INTRODUCTION

This paper reported synthesis method and characterization of Y_2O_3: Dy^{3+} phosphors. Yttrium oxide (Y_20_3) is one of the best hosts for rare earth ions because of the similarities in the chemical properties and the ionic radius of rare earths. Moreover, Y_20_3 possesses a higher melting point (2400 ◦C), higher thermal conductivity, wide transparency range (0.2 – 8 μm) with a band gap of 5.6 eV, high refractive index (∼1.8) and low cut-off phonon energy (380 cm−1) ,While the majority of the works on nanocrystalline. Y_2O_3 has undoubtedly been focused on the yellow-emitting phosphors due to its unique spectral properties and has been extensively studied in various hosts. Y_2O_3: Dy^{3+} (0.5,1,1.5 mol%) phosphors were prepared by the solid state reaction method .

The structural properties of samples were investigated by using X-ray diffraction (XRD), scanning electron microscopy (SEM). The effects of Dy^{3+} concentration on the Thermo luminescence properties of Dy^{3+} doped Y2O3 nanoparticle were investigated by using TLD reader . There has been intense interest in the investigation of ultrafine fluorescent materials recently for both fundamental research and potential applications in security labeling, UV and IR radiation detectors, bioimaging, display devices, lamps and solar cell panels [1–5]

II. EXPERIMENTAL METHODS

2.1 Sample Preparation

Analytical grade Y_20_3 (99.9%), dysprosium oxide (Dy_20_3; 99.9%), were purchased from Sigma-Aldrich Corporation,where Y2O3 was used as raw material for the host whereas dysprosium oxide (Dy_20_3) was taken as activator. Phosphor precipitates were synthesized by the solid state reaction method .They were weighed in appropriate compositions. Keeping the co-dopant Dy^{+3} concentrations varied in sample as 0.5,1,1.5,2mol%.

The composite powders were grounded in an agate mortar and pestle for about half an hour and then placed in an alumina crucible[11]. After the powders has been sintered at 1200^{0}C for 3 hr in a muffle furnace with a heating rate of 5^{0}C/min the same was cooled to room temperature. All the samples were again grounded into fine powder using an agate mortar and pestle about half an hour[15].

2.2 Sample Characterization

i). X-ray diffractogram is recorded in a wide range of Bragg angle 2 theta (20-80^0) using a Bruker D8 Focus XRD measuring instrument with CuCα target radiation (Bruker LynxEye detector).

ii). The morphology and crystallite size of the phosphors were determined by a Scanning Electron Microscopy (SEM). (Zeiss Sigma VP FEG SEM Instruments, Oxfordshire, UK)

iii). The Fourier transform infrared (FTIR) spectra were recorded in the wave number range 4000–400 cm^{-1} using a spectrometer (FTIR spectra recorded using Bruker, Germany (Model 3000 Hyperion Microscope with Vertex 80 FTIR System).

iv) The Thermoluminescence studies were carried out on a TLD reader I1009 (supplied by Nucleonix Sys. Pvt. Ltd. Hyderabad) after irradiation by UV-ray[15-25].

2.3 Results and Discussions

2.3.(i) X-ray diffraction: Figure 1 shows the X-ray diffraction pattern of Dy^{3+} doped Y2O3 phosphors. The XRD peaks of the virgin phosphor were identified and indexed according to the JCPDS file No. 83-0927 of Y2O3 [11].

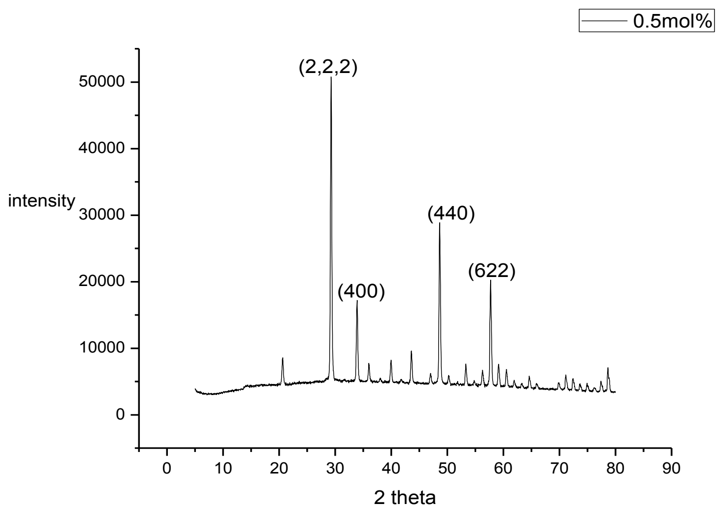

Figure 1:XRD pattern for Y2O3: Dy^{3+}

X-ray diffraction patterns taken within the 2θ scan range of 20 – 80° for the Y_2O_3: 0.5mol % of Dy^{3+}. The result shows that all diffraction peaks of these samples can be assigned to the pure-cubic structure (JCPDS 86-1107) because the crystal symmetry depends on the concentration of the doping ions, the Y2O3 cubic structure's overall peak intensity obviously decreases with increasing Dy3+ concentration in the Nanoparticles .

Debye-Scherer's equation:

IJARSE
ISSN 2319 - 8354

$$D = K\lambda/\beta \cos\Theta,$$

where K = 4/3 in the case of a spherical shape, D is the crystallite size (in ˚A), λ is the wavelength of the Cu Kα radiation(1.54˚A), and β is the corrected half width full maxima of the diffraction peak. The strongest Y2O3: 0.5% Dy+3 peak at 29.33◦ (222) was selected and yielded a calculated average size of 143.1 nm, which means that synthesized nanophosphor s actually consisted of more smaller crystallites.

2.4 Scanning Electron Microscope (SEM)

Fig. 2 shows SEM images of prepared phosphors for different resolutions. As this figures shows, the grain size of Y_2O_3: Dy^{3+} to be in the range of few microns. The surface morphology is uniform. Agglomeration of a few particles form nano-particle type of structure. Some of them were found to possess spherical shape in surface morphology of prepared phosphors which shows the cubic structure and good agreement with XRD results. The photographs of the samples show near spherical morphology with average sizes of around 110 nm.

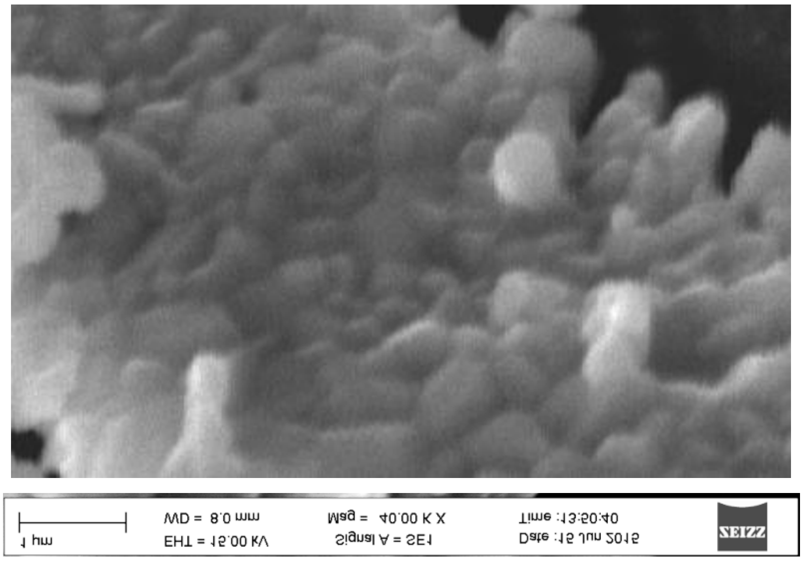

Figur2 : SEM image of Dy^{3+} (0.5mol %) with respect to resolution power 40000k.

2.5 (iv) Fourier transform infrared spectroscopy

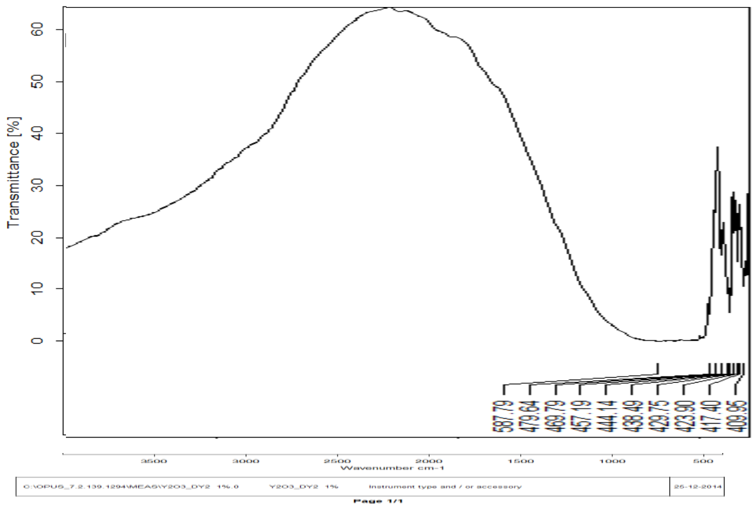

International Journal of Advance Research in Science and Engineering
Vol. No.4, Special Issue (01), September 2015
www.ijarse.com
IJARSE
ISSN 2319 - 8354

Figure 3: FTIR spectra of Y_2O_3:Dy doped phosphor

In FTIR spectra, strong peaks were centered at 409-479 cm-1 is due to Y-O vibration in the prepared sample. The broad peak centered at 587cm^{-1} is due to Dy-O vibration in the sample. The FTIR spectra also confirms the formation of Y2O3 doped with Dy phosphor prepared by solid state reaction method.

S.No.	Peak	FTIR bending/streching/vibration
1.	409-479	Y-O vibration
2.	587	Dy-O vibration

2.6 (v) Thermo Luminescence study of Y_20_3:Dy^{+3}

TL is one of the possible ways to estimate the trap states of the material. Shape factor is calculated using peak shape method. The afterglow of any phosphor is generated by the detrapped carriers that recombine with the opposite carrier in the luminescent center with a transition resulting in visible region. Y_20_3:Dy^{+3} doped with Dy^{+3} with concentration ratio 0.5 to 2 mol%, respectively, was used to undertake the TL measurements because we observed maximum TL signal strength at this ratio.

The thermoluminescence studies were carried out using TLD reader I1009 supplied by Nucleonix Sys. Pvt. Ltd. Hyderabad.

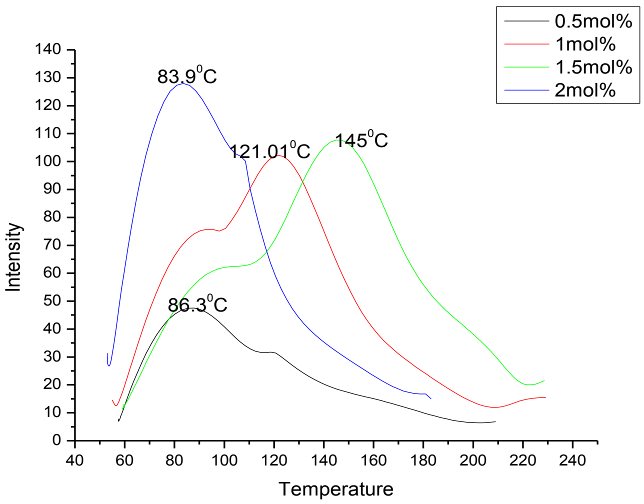

Fig. 4. TL glow curve of Dy^{+3} doped Y_20_3 phosphor variation with Dy^{+3} concentration for 5 min UV.

Figure 4 shows TL glow curves for the Dy^{+3} doped Y_20_3 phosphor exposed to 5 min dose of UV rays with 254 UV source. The variation of TL glow peak intensity as a function of Dy^{+3} concentrations was studied. The presence of Y_20_3 rare earth ions changes the TL glow curve structure either enhancing/quenching the TL efficiency. We got the maximum peak at 145^{O}C.

Peak shape method is used to determine the order of kinetics of TL glow curves so as to determine suitability of the phosphor for long afterglow. In Fig. 2 ,$\omega=\tau+\delta$; δ is the high temperature half width, τ is the low temperature

IJARSE
ISSN 2319 - 8354

half width μ_g is shape factor, Tm is the peak temperature at the maximum, and T1 and T2 are, respectively, the temperatures on either sides of Tm, corresponding to half intensity.

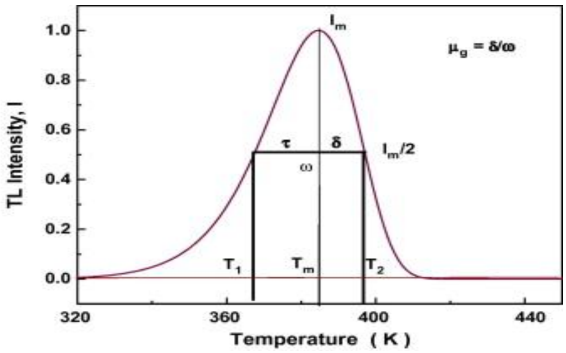

Figure 5: The characteristics points on a TL glow-peak, which define the peak-shape parameters.

The general form of the peak shape methods given by Chen is

$$E\alpha = C\alpha\ (kT^2_m/\alpha) - b_\alpha\ (2kT_m)$$

S.N0	concentrations of Dy^{+3}	T_m (^{0}C)	T_1 (^{0}C)	T_2 (^{0}C)	ω (^{0}C)	T (^{0}C)	δ (^{0}C)	μ_g (^{0}C)	Activation energy E_α (in e V)
1	0.5mol%	88	66	127.55	22	61.2	39.2	0.64	2.02
2	1 mol%	122.37	71.5	152.7	50	82.1	30.4	0.37	1.67
3	1.5mol%	147.06	115.02	173.9	32.04	58.8	26.84	0.45	2.42
4	2 mol%	122.2	71.5	152.1	17.2	47	30	0.63	2.12

Table 1: Calculation of kinetic parameters for Y_20_3: Dy^{+3} with the variation of Dy^{+3}concentration (0.5to 2 mol%) and heating rate ($5^0C\ s^{-1}$).

According table 1 the evaluated kinetic parameters shows the second order glow peaks for the different concentration effect of Dy^{+3}. The evaluated kinetic parameters shows the second order glow peak the activation energy ranging in between 1.62 to 2.42eV for most of the peaks.

The TL glow curve is related to the trap levels lying at different depths in the band gap between the conduction and the valence bands of a solid. These trap levels are characterized by different trapping parameters such as trap depth, order of kinetics, and frequency factor[26] . The loss of dosimetry information stored in the materials after irradiation is strongly dependent on the position of trapping levels within the forbidden gap which is known as trap depth or activation energy (E). The mechanism of recombination of detrapped charge carriers with their counter parts is known as the order of kinetics. The frequency factor (s) represents the product of the number of times an electron hits the wall and the wall reflection coefficient, treating the trap as a potential well. Thus, liable dosimetry study of thermo luminescent material is based on its trapping parameters.

International Journal of Advance Research in Science and Engineering
Vol. No.4, Special Issue (01), September 2015
www.ijarse.com
IJARSE
ISSN 2319 - 8354

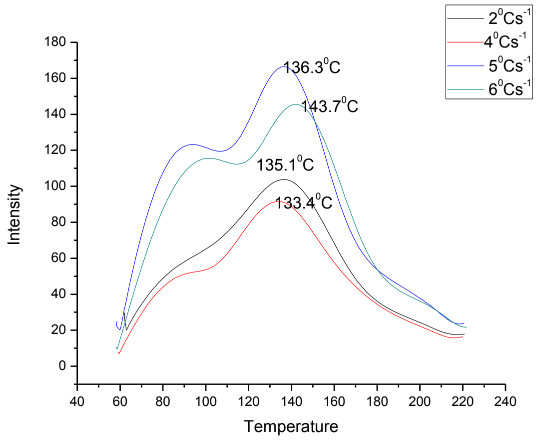

Fig. 6. TL glow curve of Dy^{+3} doped Y_20_3 phosphor variation with different heating rate.

Figure 6 shows the effect of heating rate on TL glow curve of Y_20_3: Dy^{+3} (0.5 mol%). As the heating rate increases TL peak shift towards higher temperature side, as known phenomena increasing temperature increase intensity.

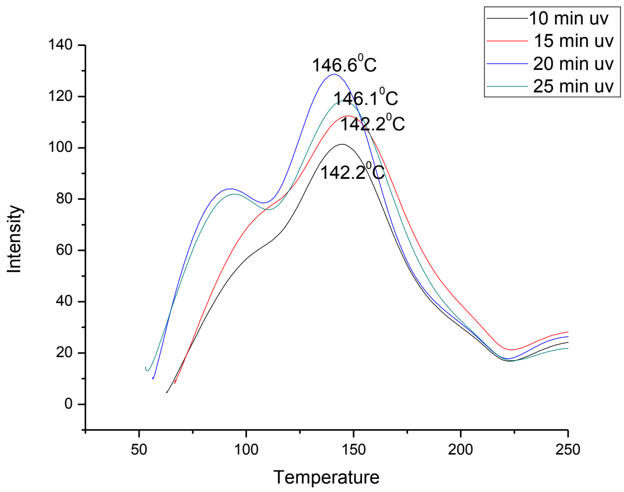

Fig. 7. TL glow curve of Dy^{+3} doped Y_20_3 phosphor variation with UV exposure time.

Figure 7 shows the effect of UV dose on TL intensity for 0.5 mol% Dy^{+3} doped Y_20_3 .It shows(Fig. 7) that the TL intensity increases linearly. It was observed that TL intensity was found to increase almost linearly with UV irradiation. Further, there was no appreciable shift in the glow peak position for higher irradiation doses. It is predicted that with the increasing UV exposure greater number of charge carriers are released which increases the trap density, results in increase of TL intensity, but after a specific exposure traps starts to destroy results in decrease in TL intensity.

III. CONCLUSIONS

Y_2O_3 phosphor co-doped with Dy^{3+}phosphor powders was successfully synthesized by the high temperature solid state reaction method. In the X ray spectra ,we got different peaks corresponding to 2θ where the highest peak refers to the 29.3^0 (222,) hkl values show the phosphor have cubic structure according to crystalline symmetry. SEM figures show, the grain size of Y_2O_3: $Dy^{3+}$is in the range of few microns .The surface morphology is uniform. The absorption band is observed around 570 cm^{-1} is because of characteristic metal-oxide (Y-O) stretching vibrations in cubic Y2O3. The evaluated kinetic parameters show the second order glow peaks for the different concentration effect of Dy^{+3}. We used the peak shape method for evaluating kinetic parameters which shows the second order glow peak because activation energy ranges between 1.62 to 2.42eV for most of the peaks . TL glow curve (figure 4) shows the variation of different concentration of Dy^{+3}. If we increase the concentration of Dy^{+3}(as activator) the TL efficiency also increases because the electrons take more energy compared to what they release. Figure (6) shows the variation of different heating rates. As the heating rate increases TL peak shifts towards higher temperature side, as increasing temperature increases intensity. Figure(7) shows the variation of different UV exposure time with respect to intensity. If UV exposure time is greater then larger number of charge carriers are released which increases the trap density and results in increase in TL intensity, but after a specific time, exposure traps start to get destroyed which results in decrease in TL intensity. Finally, we conclude that this phosphor has thermal stability and nano structure.

REFERENCES

[1] B. S. Richards, Sol. Energy Mater. Sol. Cells **90**, 1189(2006).

[2] G. K. Das and T. T. Y. Tan, J. Phys. Chem. C **112**,11211 (2008).

[3] Y. B. Mao, J. Y. Huang, R. Ostroumov, K. L. Wang andJ. P. Chang, J. Phys. Chem. C **112**, 2278 (2008).

[4] R. Kubrin, A. Tricoli, A. Camenzind, S. E. Pratsinis andW. Bauhofer, Nanotechnology **21**, 225603 (2010).

[5] F. Zhang and S. S. Wong, ACS Nano **4**, 99 (2010).

[6.] H. Eilers, B.M. Tissue, Chem. Phys. Lett. 251, 74 (1996)

[7]. M. Kottaiswamy, D. Jeyakumar, R. Jagannathan, M. Mohan Rao, Mater. Res. Bull. 31, 1013 (1996)

[8]. B. Bihari, H. Eilers, B.M. Tissue, J. Lumin. 75, 1 (1997) .

[9] T. Ye, Z. Guiwen, Z. Weiping, X. Shangda, Mater. Res. Bull. 32, 501 (1997)

[10]. F. Wang, Y. Han, C.S. Lim, Y. Lu, J. Wang, J. Xu, H. Chen, C. Zhang, M. Hong, X. Liu, Nature 463, 1061–1065 (2010)

[11]. R.D. Shannon, Acta Crystallogr. Sect. A 32, 751–767 (1976)

[12]. M. Maestro, D. Huguenin, A. Seigneurin, F. Deneuve et al., J. Electrochem. Soc. 139(5), 1479 (1992)

[13].. X.R. Hou, S.M. Zhou, H. Lin, H. Teng, Y.K. Li, W.J. Li, T.T. Jia, J. Appl. Phys. 107(8),083101 (2010)

[14] L.O.O. Costa, A.M. Silva, L.E.P. Borges, L.V. Mattos, F.B. Noronha, Catal. Today 138(3–4), 147(2008)

[15]. A.M. Edwin Suresh Raj, C. Maria Magdalane, K.S. Nagaraja, Phys. Status Solid 191(1), 230 (2002) 8. G.K. Das, T.T.Y. Tan, J. Phys. Chem. C 112(30), 2009.

[16] Z. Xiao, Y. Lu, F. Zhu, F. Zhang, A. Huang and P. Yin, J. Korean Phys. Soc. **55**, 6 (2009).

[17] S. Seo, H. Yang and P. H. Holloway, J. Colloid Interface Sci. **331**, 236 (2009).

[18] S Agrawal, V Dubey, 3rd international conference on fundamental and applied sciences (icfas 2014): Innovative Research in Applied Sciences for a Sustainable Future, 1621, 560-564, http://dx.doi.org/10.1063/1.4898522.

[19] V Dubey, J Kaur, S Agrawal, Research on Chemical Intermediates 41 (1) 2014, 401-408.

[20] VikasDubey, JagjeetKaur, SadhanaAgrawal, Materials Science in Semiconductor Processing 31 (2015) 27–37.

[21] VikasDubey, SadhanaAgrawal, JagjeetKaur, Optik 126 (2015) 1–5.

[22] C. Hu, H. Liu, W. Dong, Y. Zhang, G. Bao, C. Lao, Z.L. Wang, Adv. Mater. 19 (2007) 470–474.

[23] VikasDubey, V.P. Dubey, Raunak Kumar Tamrakar, KanchanUpadhyay, NehaTiwari, Journal of Radiation ,Research and Applied Sciences, Volume 8, Issue 1, January 2015, Pages 126-135.

[24] R Shrivastava, J Kaur, V Dubey, B Jaykumar, S Loreti, Spectroscopy Letters 48 (3) 2014, 179-183.

[25] V Dubey, R Tiwari, RK Tamrakar, GS Rathore, C Sharma, N Tiwari, Infrared Physics & Technology 2014 67, 537-541.

[26] Wikipedia and free encyclopedia

[27] J L mer P S Persian Phys. Rev. **162** 217 (1967)

[28] F K Fong J. Chem. Phys. **41** 245 (1964)

[29] C M Sunta Radiat. Prot. Dosim. **8** 25 (1984)

[30] V R Mathur In: Thermoluminescent Materials, Ed D.R. Vij (Prentice Hall, Englewood Cliffs, N J) p. 181 (1993)